NUCL SCI TECH (2019) 30:144
https://doi.org/10.1007/s41365-019-0655-6

Touschek lifetime study based on the precise bunch-by-bunch BCM system at SSRF

Fang-Zhou Chen[1,2] · Zhi-Chu Chen[2,3] · Yi-Mei Zhou[1,2] · Ning Zhang[2,3] · Bo Gao[2,3] · Xing-Yi Xu[1,2] · Yong-Bin Leng[1,2,3]

Received: 28 January 2019 / Revised: 30 April 2019 / Accepted: 5 May 2019 / Published online: 24 August 2019

Abstract Continuous tracking of bunch charges is the key to maintain stable operations in a storage ring in top-up mode. Recently, a precise bunch-by-bunch beam-current measurement (BCM) system has been developed at the Shanghai Synchrotron Radiation Facility. To avoid the influence of longitudinal oscillation on the amplitudes of the sampling points, a method called two-point equilibrium sampling is introduced. The results, obtained during routine operation time, show that the relative resolution of the measurement of the bunch charges is better than 0.02%. With this high resolution, the new BCM system is able to monitor the bunch-by-bunch beam lifetime. By using the filling pattern information, the Touschek lifetime and the vacuum lifetime can also be calculated. In this paper, the principle of the new method and the experiments is presented in detail.

Keywords Beam-current measurement · Bunch-by-bunch · Touschek lifetime · Vacuum lifetime · SSRF

This work was supported by the National Natural Science Foundation of China (No. 11575282) and the Ten Thousand Talent Program.

✉ Yong-Bin Leng
lengyongbin@sinap.ac.cn

1 Shanghai Institute of Applied Physics, Chinese Academy of Sciences, Shanghai 201800, China

2 University of Chinese Academy of Sciences, Beijing 100049, China

3 Shanghai Advanced Research Institute, Chinese Academy of Sciences, Shanghai 201200, China

1 Introduction

The Shanghai Synchrotron Radiation Facility (SSRF) is a multi-bunch, high-current, advanced third-generation synchrotron light source. The main parameters of its storage ring are listed in Table 1.

The beam current and its lifetime are two of the most important parameters of an electron storage ring. They are used to not only characterize the beam quality and machine status, but also to quantify the injection efficiency for weighing the injector/storage-ring matching.

The average beam current is measured to control injections during top-up operations, calculate the average lifetime and stability of the beam, and calculate the injection efficiency to determine whether the beam loss during an injection is tolerable. The charges of the bunches are used to check the filling pattern and determine how to make the next injection to achieve the designed pattern, such that the desired filling pattern and the operation mode can be sustained.

There might also come a situation in which the values of the Touschek lifetime, vacuum lifetime, and quantum lifetime are needed, especially during machine studies.

When a sudden beam loss occurs, the total and the individual charge reductions are both needed to analyze the root cause of the accident and to further optimize the performance.

The average beam current is usually picked up by a new parametric current transformer (NPCT; sometimes called a DC current transformer, DCCT). Combining with a narrow-banded and high-resolution digital acquisition device, this beam-current measurement (BCM) system can operate with the resolution of better than 2μA at a refresh rate

Table 1 Main parameters of the SSRF storage ring

Parameter	Value
Beam energy (GeV)	3.5
RF frequency (MHz)	499.654
Current (mA)	240
RF harmonic number	720
Filled buckets	500
Bunch charge (nC)	0.3–1.0
Bunch length (ps)	14.4
Longitudinal tune	0.007
Timing trigger rate (Hz)	2

greater than 1 Hz, when the dynamic range is approximately 2A [1–4].

However, owing to the diversity among the bunches, the average is not sufficient to describe the behavior of all the bunches in the storage ring individually and accurately. The lifetime formulae can only be strictly applied to a single bunch; in terms of the multi-bunch situation, the lifetime can only be calculated using approximate parameters. The information of the average beam current is not good enough to analyze and locate the source in the case of beam loss. Moreover, the Touschek lifetime and the vacuum lifetime analysis using the average beam current require a larger range of beam currents (on the order of tens of mA), as well as a longer acquisition time (on the order of hours). In addition, this kind of average algorithm is unable to detect fast changes in bunch lifetimes. Thus, it is difficult to make DCCTs useful in cutting-edge research.

There are two common types of bunch-by-bunch charge-measurement systems, or filling pattern-monitoring systems, in an electron storage ring. The conventional type picks up the bunch signals with four button-type electrodes of a beam position monitor (BPM). After the radio-frequency (RF) signals pass through the signal conditioning front end, which consists of a variety of phase-stable cable assemblies, broadband signal synthesizers, and low-pass or band-pass filters, they are recorded by a high-speed broadband digitizing module. This type of bunch-by-bunch charge-measurement system can be seen at the National Synchrotron Light Source II (NSLS II), Beijing Electron-Positron Collider II (BEPC II), and SSRF [5–8].

The other type picks up the synchrotron radiation of each bunch with photodiodes in a diagnostic beam line. After being conditioned at the front end with RF amplifiers and low- or band-pass filters, the signals are also recorded by a high-speed broadband digitizing module, as in the conventional method. This type of bunch-by-bunch charge-measurement system can be seen at the Australian Synchrotron (AS), the Swiss Light Source (SLS), and the Hefei Light Source II (HLS II) [9–11]. This type was designed initially to achieve a relative resolution of 0.1% at a refresh rate of greater than 1 Hz when the dynamic range is of the order of 1 nC.

The beam instrumentation group at the SSRF has focused on the study of bunch-by-bunch beam diagnostics since 2009 [12–18]. It has been proven that the BCM system can achieve a resolution of 0.1% with the single-point sampling method [7, 8, 19]. However, additional system offsets may increase owing to phase drifting during long-term operation. On this basis, the phase-equilibrium sampling method has been created to enhance the BCM system accuracy, stability, and reliability. The new BCM system can achieve high-speed bunch-by-bunch lifetime measurement. The bunch charges in the SSRF storage ring are not uniformly distributed. By taking advantage of the variation in the bunch charges, we can measure the Touschek lifetime and perform vacuum lifetime analysis.

This paper reviews previous bunch-by-bunch measurement works and focuses on the beam-lifetime measurement. The remainder of this paper is organized as follows: The fundamental physical principles are presented in Sect. 2. The method is introduced in Sect. 3. Next, beam experiments and results are discussed in detail in Sect. 4. The conclusion is given in Sect. 5.

2 Basic principle

When a four-electrode BPM is used, the sum signals of all electrodes are proportional to the bunch charges under paraxial approximation [5, 19–21]. Therefore, they can be used to calculate the lifetimes of all bunches.

The lifetime of a bunch is determined by three mechanisms: the quantum excitations, intra-bunch scatterings, and bunch-gas scatterings [22]. They are called the quantum lifetime, Touschek lifetime, and vacuum lifetime, respectively [23, p. 388, p. 394, p. 431, & p. 705].

$$\begin{aligned}
\tau_{\mathrm{q}} &= \frac{1}{2}\tau_w \frac{e^{\xi}}{\xi}, \quad \text{where } \xi = \frac{A^2}{2\sigma^2} \\
\tau_{\mathrm{T}}^{-1} &= \frac{r_{\mathrm{c}}^2 cN}{8\pi\sigma_x\sigma_y\sigma_\ell}\frac{\lambda^3}{\gamma^2}D(\epsilon) \\
\tau_{\mathrm{cs}}^{-1} &= c\beta 2\mathcal{A}\frac{P[\mathrm{Torr}]}{760}\left(\frac{zZe^2}{2\beta cp}\right)^2\frac{4\pi}{\tan^2(\hat{\theta}/2)} \\
\tau_{\mathrm{bs}}^{-1} &= -\frac{4}{3}c\sum_i \frac{1}{760}\frac{\tilde{P}_i[\mathrm{Torr}]}{L_{r,i}}\ln\delta_{\mathrm{acc}}
\end{aligned} \tag{1}$$

They are so well known in the particle physics field that descriptions and explanations of the individual parameters are trivial. Only the parameters of interest will be discussed here.

The total loss rate is the sum of all loss rates:

$$\tau^{-1} = \tau_{\mathrm{q}}^{-1} + \tau_{\mathrm{T}}^{-1} + \tau_{\mathrm{cs}}^{-1} + \tau_{\mathrm{bs}}^{-1}, \quad (2)$$

where τ_{q}, τ_{T}, τ_{cs}, and τ_{bs} are the quantum lifetime, Touschek lifetime, vacuum lifetime owing to Coulomb or elastic scattering, and vacuum lifetime owing to bremsstrahlung or inelastic scattering, respectively.

The quantum lifetime τ_{q} is related to the aperture A and the bunch size σ. A is much greater than σ in design, so the quantum lifetime is too long to have any effective influence on the total lifetime [22]. However, when A shrinks in some cases and becomes comparable to σ, the quantum lifetime will exponentially decrease and the loss rate owing to quantum excitation will be visible.

The vacuum lifetimes τ_{cs} and τ_{bs} are proportional to the residual gas pressure P or $\tilde{P}_i$, regardless of the collision mechanism. They are also affected by the β function and the 3D acceptance $\hat{\theta}$ and δ_{acc} [24]. During the operation in a third-generation synchrotron radiation facility with designed parameters, the residual gas pressure in the vacuum pipe decreases gradually, so the vacuum lifetime $\tau_{\mathrm{v}} \equiv (\tau_{\mathrm{cs}}^{-1} + \tau_{\mathrm{bs}}^{-1})^{-1}$ increases along with the decrease in the residual gas pressure until it approaches a constant at the leakage-pumping equilibrium. The vacuum lifetime is much longer than the Touschek lifetime under good vacuum conditions. However, changes in any of the related parameters will directly cause changes in the vacuum lifetime, so the vacuum lifetime can be used to indicate the overall stability of the storage ring. For example, if the vacuum lifetime is being measured on line, the ring stability can be evaluated with this single parameter, and predictions can be made before the machine is out of control.

The Touschek lifetime τ_{T} is related to the bunch charge $Q = eN$, the 3D bunch sizes σ_x, σ_y and σ_ℓ. All the above parameters are characteristics of an individual bunch. If anything happens, e.g., beam instabilities or turbulences of RF parameters, and the bunch size changes, the Touschek lifetime will also change accordingly. Therefore, the Touschek lifetime, or the normalized Touschek factor with respect to the bunch charge, can be used to indicate the stabilities of the bunches. If the Touschek factor is being measured on line, the bunch stability can be evaluated with the single factor, and prediction can be made before the beam is out of control.

By analyzing the lifetime expressions, one can find that the quantum lifetime and the vacuum lifetimes are irrelevant to the bunch charge, but the Touschek lifetime is linearly correlated to it. If the charges of all bunches are not identical, by measuring the lifetime of each bunch quickly and precisely, we can obtain the Touschek factor with linear regression analysis [25]:

$$\frac{1}{\tau_i} = \kappa Q_i + \frac{1}{\tau_0}, \quad (3)$$

where τ_i is the calculated total lifetime of the ith bunch, Q_i is the charge of the ith bunch, $\tau_0 = (\tau_{\mathrm{q}}^{-1} + \tau_{\mathrm{v}}^{-1})^{-1}$ is the combined lifetime of the vacuum lifetime and the quantum lifetime, and κ is the Touschek factor, which is proportional to the loss rate owing to the Touschek effect. When the quantum lifetime is much longer than the vacuum lifetime, τ_0 can be regarded as the vacuum lifetime τ_{v}. The quantum lifetime will from now on be ignored, especially in Sect. 3, unless otherwise noted.

3 Method

The most common way to pick up the signals from the button-type electrodes is to use a sampler whose sampling frequency equals the bunch repetition rate. By adjusting a phase shifter, the best signal-to-noise ratio can be obtained when the synchronous sampling is at the signal peaks. This method has some obstacles to overcome in this particular situation. Owing to the synchrotron dynamics, peak locations of all bunches from the electrodes will oscillate about the timing signal [24].

Before making any further progress, we had estimated the effect of the clock jitter. The timing signals from the SSRF were used as the clock to sample the signals from a waveform generator. The results showed that the jitter would contribute an error of around 40 ps to the sampling.

To minimize the system error caused by the longitudinal oscillation and the jitter of the triggers, the data acquisition system adopts a two-point equilibrium sampling method.

3.1 Idea

The purpose of the two-point sampling method is to find the peak value of the signal whenever the trigger occurs. The invoked signal is sampled at two points with fixed time delay Δt (as shown in Fig. 1). The signal $f(t)$ can be normalized to a fixed concave function $f_0(t)$ by multiplying a factor $A(Q)$ related to the bunch charge (as shown later in

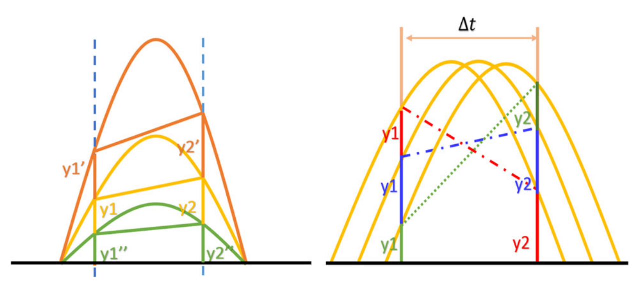

Fig. 1 Sketch map of two-point phase sampling methodology

this section). If the length of the interval between the two sample points is fixed, it can be easily seen that the concavity assures that the ratio of the values $g(t) = f_0(t)/f_0(t+\Delta t)$ at the two sample points is (strictly) monotonically decreasing. Thus, $g(t)$ is a bijective function.

Suppose the two measured values are $y_1 = f(t_1)$ and $y_2 = f(t_2) = f(t_1 + \Delta t)$. The idea is eliminating the factor by dividing the two values, and using the injection property of $g^{-1}(t)$ to get the phases of the two points. We can even make a new function $V(y_1, y_2)$ that outputs the bunch charge. The function is discrete, so interpolation might be necessary in practice.

3.2 System setup

The layout of the measurement system is shown in Fig. 2. It consists of three major components: the front-end electronics, the fast digitizer (a high-speed ADQ card), and the timing system. The front-end electronics handles the four signals of each bunch, via phase shifters to compensate phase shifts caused by the transmission cables, and then transmits the signals into the signal combiner. After that, the sum signals are divided into two channels with a Mini-Circuits power splitter ZFSC-2-372-S+. The two channels of the sum signals are transmitted, via two high-precision delay cables whose phase difference is strictly 100 ps, into the two channels of the SP devices ADQ14 digitizer card (external clock 999.63 MHz, external triggered at 2 Hz, 14 bits ADC) [26]. The front-end electronics is equipped in the tunnel of the accelerator to reduce the reflections due to impedance mismatches.

The timing system consists of a trigger signal and a clock signal. The sampling clock uses the main accelerator clock directly to guarantee the sampling synchronicity. A phase shifter is used to adjust the ADC sampling clock to find the peak value of the sum signal.

The acquisition routine is as follows: Both channels will acquire approximately 1000 turns of bunch-by-bunch data simultaneously. Each channel (separated by 100 ps) will take one sample at a bucket every turn. The two data stream will be zipped with the bunch charge function $V(y_1, y_2)$, and we will obtain 1000 turns of the peak voltages of all bunches. Taking the averages along the turns, we can get the mean voltages of all bunches. The bunch charges are calculated by multiplying a coefficient that was calibrated with an NPCT.

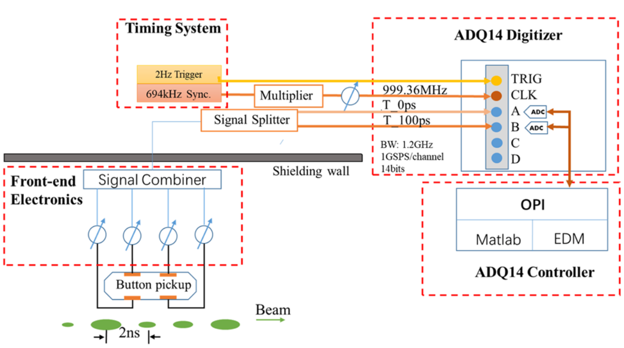

Fig. 2 System layout of two-point phase sampling method

3.3 Response waveform reconstruction

To calibrate the function $g(t) = f(t)/f(t+\Delta t)$, we measure the waveforms of the sum signals. Each bunch lasted 2 ns and the concavity changes at the zero-crossing point.

The same layout of the acquisition system, as shown in Fig. 2, was used to reconstruct the response signal of a passing bunch. The sampling frequency of the ADQ card is 1 Gigabit Samples Per Second and the bandwidth of the ADQ card is 1.2 GHZ, so each sampling clock can only acquire two samples for the sum signal of the bunch. Under this consideration, we use the high-precision NARDA-ATM coaxial phase shifter P1100D [27]. The adjustable group delay ranges from 0 to 1.016 ns. The phase shifter is controlled by a multi-turn non-translating shaft, with approximately 100 turns from minimal to maximal phase adjust. With this high-precision phase shifter, we can reconstruct the refined waveform of the sum signal.

To check the consistency and to reduce the random noise, we normalized the waveforms of all the filled bunches and obtained the response function by averaging and interpolation. It is safe to say that in the interval around the peak, the waveform is a concave function.

3.4 Bunch charge calculation

To calibrate the relation between the bunch charge and the two measured voltages separated by a fixed time interval, we pick the delay line $\Delta t = 100\,\text{ps}$ and use the reconstructed waveform to calculate the relation curve.

Because t_1 can be seen as a function of $f_0(t_1)/f_0(t_1+\Delta t) \equiv f(t_1)/f(t_1+\Delta t)$, the peak V is uniquely determined. We have further calibrated the coefficient K as a function of $f_0(t_1)/f_0(t_1+\Delta t)$ where the peak $V = Kf(t_1)$.

3.5 Bunch charge measurement resolution evaluation

As soon as we obtained the function to calculate the bunch charge, the first experiment was to evaluate the jitter, the longitudinal oscillation, and the readout errors (as shown in Fig. 3). The raw signals of the two channels separated by 100 ps were recorded at a regular stored bunch

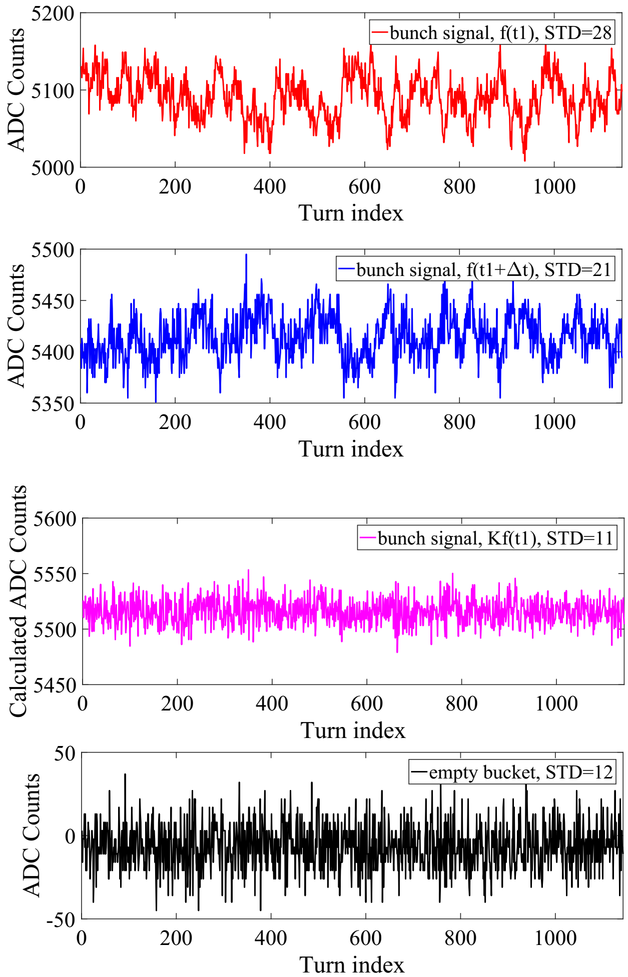

Fig. 3 Readout noise evaluation. Red and blue lines: raw readouts of the two channels; magenta: calculated readouts of peak values; and black: raw readouts of background noise

and at an empty bucket. The latter signals could be regarded as pure readout errors, and the former signals contain the effects of the jitter, the synchrotron motions in addition to the ADC readout.

The ADC readout noise of the empty bucket is approximately 12 and the total measurement variation is approximately 21 (close to peak) or 28 (away from peak), so the measurement error introduced by the jitter and the synchrotron oscillation is approximately $\sqrt{21^2 - 12^2} \simeq 17$ or $\sqrt{28^2 - 12^2} \simeq 25$, depending on where the measurement occurs. This is expected, given that the slope differs at different phases. The two-point method could efficiently reduce the measurement error. The relative resolution is 0.2%. The stochastic noise can be reduced by averaging all the samples (approximately 1000 turns) taken after a timing trigger (2 Hz).

Another experiment was also conducted to evaluate the performance of this method. The new system is expected to have a finer resolution than that of the traditional method, i.e., taking just one sample around the peak.

Two series (separated by 100 ps) of bunch signals were taken, and the "actual" charges were calculated with them. We can see that the signal contains the decay of the bunch charge and all kinds of noises. We assumed a linear approximation of decay of the bunch in a short period for simplicity. After removing the "theoretical" decay, we got the standard deviation $\sigma = 0.14\,\mathrm{pC}$ of what is left. That value was regarded as the maximal system resolution. Given that the bunch charge was approximately 950 pC, the relative measurement resolution is better than 0.02%, which is approximately five times better than the former BCM system [7, 8].

3.6 Beam-lifetime analysis method

The new BCM system is now ready to measure the bunch-by-bunch beam lifetime with high precision. This enables us to analyze the Touschek lifetime and the vacuum lifetime on a finer scale.

Because the Touschek lifetime is dominated by the intra-bunch scattering effect, the lifetime of each bunch varies with its charge. We have recorded the raw data of all the storage bunches of the whole storage ring between two injections and calculated the lifetimes of all bunches. The loss rate, i.e., the reciprocal of the lifetime, is linearly related to the bunch charge (as shown in Fig. 4). The Touschek factor and the vacuum lifetime can be directly obtained by using Eq. (3). In this case, the vacuum lifetime is $\tau_{\mathrm{vacuum}} = (35.8 \pm 0.1)\,\mathrm{h}$ and the Touschek factor is $\kappa = (0.0248 \pm 0.0001)\,\mathrm{h}^{-1}\ \mathrm{nC}^{-1}$.

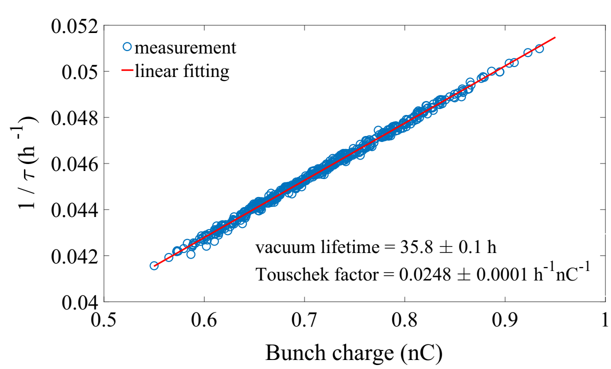

Fig. 4 The correlation between reciprocal of beam lifetime and bunch charge

4 Applications

This system intends to work during normal operations for users (top-up mode at 240 mA), user studies, or machine studies. The physical aperture is one of the most convenient parameters to adjust. Thus, an experiment was arranged and a scraper was available to simulate the change in the acceptance of the beam transporter.

Meanwhile, a miniscule beam loss was noticed by the system during a normal top-up operation, and the cause of the event was roughly categorized for further analysis.

4.1 Study of the physical aperture

Collimators and scrapers are used to select a portion of the beam by blocking or deflecting the unwanted electrons. The locations of the blades determine the physical aperture at that position of the vacuum chamber. Because they can provide some reliable data, they are still worth studying.

As can be seen in Eq. (1), all the lifetimes are determined by the acceptance of the beam transport line. The Touschek lifetime τ_T is proportional to the cube of the momentum acceptance λ^{-1}. Moving the scraper transversely in a dispersive section will also affect the momentum acceptance. The blade in this experiment could move very close to the bunch center, invalidating the enormously long quantum lifetime assumption. Thus, the combined vacuum and quantum lifetimes should be considered. This combined lifetime is more complicated, so we can only expect to see that τ_0 and the gap size are positively correlated.

An experiment was designed to observe the relation between the lifetime and the physical aperture. We changed the gap of a vertical scraper and measured the bunch-by-bunch charges.

No obvious changes in the normalized filling pattern were observed when the blades were moved closer. Thus, beam loss due to instabilities can be ignored. After separating the Touschek lifetime via Eq. (3), we can check the relation between the lifetimes and the physical aperture.

The gap was initially set to 8 mm, and the corresponding Touschek factor $\kappa = \tau_T^{-1}/Q$ was $0.039\,\mathrm{h}^{-1}\ \mathrm{nC}^{-1}$, and the residual lifetime τ_0 was 32.7 h. When the gap was shrunk to 7.5 mm, 7.0 mm, 6.0 mm, and 5.0 mm, the Touschek factor became $0.04\,\mathrm{h}^{-1}\ \mathrm{nC}^{-1}$, $0.053\,\mathrm{h}^{-1}\ \mathrm{nC}^{-1}$, $0.068\,\mathrm{h}^{-1}\ \mathrm{nC}^{-1}$, and $0.225\,\mathrm{h}^{-1}\ \mathrm{nC}^{-1}$, respectively. The residual lifetime slowly decreased with the gap at first and then suddenly dropped, much faster than the Touschek lifetime, until it reached 1.8 h.

The Touschek lifetime $\tau_T \propto \kappa^{-1}$ is roughly a cubic function of the gap size, based on the above data. The deviation may be introduced by measurement errors, variation in the Touschek function $D(\epsilon)$ in Eq. (1), or changes in the beam size.

The behavior of the residual lifetime suggests that the quantum lifetime, which is exponentially related to the squared aperture size as shown in Eq. (1), dominates over the vacuum lifetime later.

4.2 Analysis of accident beam loss

The high-precision BCM system can provide bunch-by-bunch beam-charge information to detect sudden beam losses, whereas a DCCT can only obtain, somewhat slowly, the average beam current.

The resolution of the old BCM system at the SSRF is approximately 0.1%. A beam loss of greater than 1 pC could be detected when the single bunch charge is approximately 1 nC. When the storage ring is evenly filled with 500 bunches, only current drop greater than $500 \times 1/1.44 = 0.34\,\mathrm{mA}$ may be visible to be located and analyzed. The resolution of this new BCM system is approximately 0.02%, which means the new BCM system can be used to analyze all current drops that are greater than $500 \times 1/1.44 = 0.07\,\mathrm{mA}$.

Normally, SSRF operates at 240 mA in top-up mode. In this research, an unexpected tiny (0.2 mA) beam loss during normal operation was observed on December 16, 2018. Using the high-precision bunch-by-bunch BCM system, we found that the bunch-charge loss had a strong correlation with the bunch charge and a weak correlation with the position in the bunch train (as shown in Fig. 5). According to accelerator physics, there are two main beam-loss classes: those due to scattering and those due to instabilities [24]. Based on this analysis, it can be inferred that the beam loss may be caused by scattering. Further studies are required for accelerator physicists to determine the beam-loss mechanics in this case.

5 Conclusion

A bunch-by-bunch BCM system, based on the BPM sum signals and the two-point equilibrium sampling method, has been developed at the SSRF to make high-precision charge measurements. The two-point equilibrium sampling method can overcome the weakness of the single-point method so that the measurement will not be affected by trigger jitter or the longitudinal dynamics of the beam. By applying this new method, the relative resolution of the measurement of the bunch charge is better than 0.02%. With this high resolution, the new system is able to monitor the bunch-by-bunch beam lifetime. By taking advantage of the variation in the bunch charges, we can achieve the Touschek lifetime and vacuum lifetime analysis. The

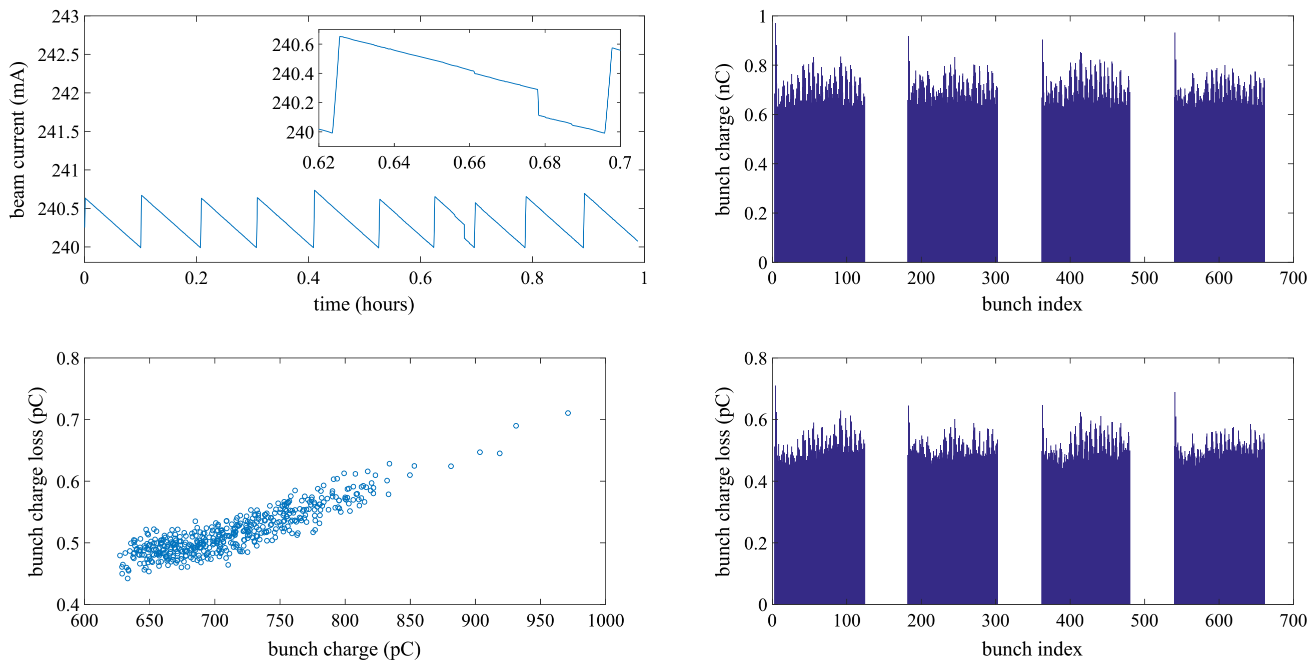

Fig. 5 Beam loss detected on December 16, 2018. Upper left: intensity fluctuations record by our DCCT, upper right: filling pattern, lower left: relation between the bunch charges and the losses, lower right: the sudden losses in different buckets

lifetime measurement will be useful for accelerator physicists when optimizing the machine with more and more IDs.

Acknowledgements The authors thank the operation team of SSRF for their assistance in conducting the beam experiment.

References

1. Y.B. Leng, W.M. Zhou, Y.Z. Chen et al., DCCT system design for SSRF storage ring. Nucl. Tech. **30**, 2 (2007)
2. E. Soliman, K. Hofmann, H. Reeg et al., in *Sensor studies for DC current transformer application*. Proceeding of 3rd International Beam Instrumentation Conference (Califonia, USA, 2014) pp. 515-520
3. Bergoz Instrumentation. New parametric current transformer user's manual. https://www.bergoz.com/files/npctmanual2-0. Accessed Mar 2018
4. Z.C. Chen, Y.B. Leng, Y. Zhou et al., Baseline recovery method to measure bunch charge under low-current mode of SSRF. Nucl. Sci. Tech. **22**, 261–264 (2011). https://doi.org/10.13538/j.1001-8042/nst.22.261-264
5. H. Yong, L. Dalesio, K. Ha et al., in *WEPKN014: NSLS- filling pattern measurement*. Proceedings of 13th Conference on Accelerator and Large Experimental Physics Control Systems (WTC Grenoble, France, 2011), pp. 735–737
6. Q.Y. Deng, J.S. Cao, J.H. Yue et al., Bunch-by-bunch beam loss monitor system in BEPC II storage ring. High Power Laser Part. Beams **26**, 105101 (2014). https://doi.org/10.11884/HPLPB201426.105101. (in Chinese)
7. Y.B. Leng, Y.B. Yan, L.Y. Yu et al., in *MOPE034: Data acquisition for SSRF ring bunch charge monitor*. Proceeding of 1st International Particle Accelerator Conference (Kyoto, Japan, 2010), pp. 1047–1049
8. F.Z. Chen, L.W. Lai, Y.B. Leng, et al., in *TUPWC03: Design of a new type of beam charge monitor based bunch-by-bunch DAQ system*. Proceeding of 6th International Beam Instrumentation Conference (Michigan, USA, 2017) pp. 284–286. https://doi.org/10.18429/JACoW-IBIC2017-TUPWC03
9. D.J. Peake, M.J. Boland, G.S. LeBlanc et al., Measurement of the real time fill-pattern at the Australian Synchrotron. Nucl. Instrum. Methods Phys. Res. Sect. A Accel. Spectrom. Detect. Assoc. Equip. **2**, 589 (2008). https://doi.org/10.1016/j.nima.2008.01.072
10. B. Kalantari, V. Schlott, T. in *Korhonen, Bunch pattern control in top-up mode at the swiss light source*. Proceedings of the EPAC 2004 (Lucerne, Switzerland, 2004), p. 2885–2887
11. T.Y. Zhou, Y. Yang, B.G. Sun et al., Beam current measurement using a high-speed photodetector at HLS II. IEEE Trans. Nucl. Sci. **7**, 64 (2017)
12. S.T. Huang, Y.B. Leng, Y.B. Yan, Development of the bunch-by-bunch beam current acquisition system at SSRF. Nucl. Sci. Tech. **20**, 71 (2009). https://doi.org/10.13538/j.1001-8042/nst.20.71-75
13. Y.B. Leng, Y.B. Yan, L.Y. Yu et al., Monitoring the charge bunch-by-bunch for the SSRF storage ring: development and application. Nucl. Sci. Tech. **21**, 193 (2010). https://doi.org/10.13538/j.1001-8042/nst.21.193-196
14. Z.C. Chen, Y.B. Yang, Y.B. Leng et al., Wakefield measurement using principal component analysis on bunch-by-bunch information during transient state of injection in a storage ring. Phys. Rev. ST Accel. Beams **17**, 112803 (2014). https://doi.org/10.1103/PhysRevSTAB.17.112803
15. Y. Yang, Y.B. Leng, Y.B. Yan et al., Development of the bunch-by-bunch beam position acquisition system based on BEEcube. Nucl. Sci. Tech. **27**, 47 (2016). https://doi.org/10.1007/s41365-016-0035-4
16. L.W. Duan, Y.B. Leng, R.X. Yuan et al., Injection transient study using a two-frequency bunch length measurement system at the SSRF. Nucl. Sci. Tech. **28**, 93 (2017). https://doi.org/10.1007/s41365-017-0247-2

17. Y.M. Zhou, H.J. Chen, S.S. Cao et al., Bunch-by-bunch longitudinal phase monitor at SSRF. Nucl. Sci. Tech. **29**, 113 (2018). https://doi.org/10.1007/s41365-018-0445-6
18. H.J. Chen, J. Chen, B. Gao et al., Bunch-by-bunch beam size measurement during injection at Shanghai Synchrotron Radiation Facility. Nucl. Sci. Tech. **29**, 79 (2018). https://doi.org/10.1007/s41365-018-0420-2
19. Y.B. Leng, Y.B. Yan, W.M. Zhou et al., Precise beam current measurement for storage ring using beam position monitor. High Power Laser Part. Beams **22**, 2973–2978 (2010). https://doi.org/10.3788/HPLPB20102212.2973. (in Chinese)
20. B.C. Zhang, Y.B. Leng, Simulation of beam bunch charge measurement using BPM pickup. Nucl. Tech. **32**, 4 (2009). (in Chnese)
21. Y. Yang, Y.B. Leng, Y.B. Yan, et al., in *MOPME054: Bunch-by-bunch beam position and charge monitor based on broadband scope in SSRF*. Proceedings of 4th International Particle Accelerator Conference (Shanghai, China, 2013), p. 595–597. http://accelconf.web.cern.ch/accelconf/IPAC2013/papers/mopme054.pdf
22. J.J. Eberhard, K. Shaukat, R.S. Jochen et al., *Synchrotron Light Sources and Free-electron Lasers* (Springer, Basel, 2016), pp. 291–293
23. H. Wiedemann, *Particle Accelerator Physics*, 3rd edn. (Springer, New York, 2007)
24. S.Y. Lee, *Acceletator Physics* (World Scientific Publishing, Hackensack, 2004), pp. 456–459
25. Z.C. Chen, Y.B. Leng, R.X. Yuan et al., Experimental study using Touschek lifetime as machine status flag in SSRF. Chin. Phys. C **38**, 7 (2014). https://doi.org/10.1088/1674-1137/38/7/077005
26. Teledyne SP Devices. ADQ14AC-4C specifications. https://spdevices.com/documents/datasheets/19-adq14-datasheet/file. Accessed 13 Apr 2018
27. NARDA-ATM coaxial phase shifter. phase-shifter P1100D. https://www.atmmicrowave.com/coaxial/phase-shifter-line-stretcher/. Accessed July 2001